An X-Band Acousto-Optic Variable Delay Line for Radar Target Simulation

Michael C. Zari, Chris S. Anderson, and Willie D. Caraway III, *Member, IEEE*

***Abstract*—The design and characterization of a 54-μs, continuously-variable, acousto-optic (AO) delay line developed for radar testing applications is presented. Design goals for the delay line include over 10 MHz of instantaneous bandwidth, 1.2 GHz of tunable bandwidth operating at X-band, 45 dB of dynamic range, and electronically-controllable delay selection to simulate dynamic radar targets with radial range rates up to 500 m/s. In addition, the device was designed to have phase noise and spurious signal levels compatible with high performance radars. To achieve these goals, a 33-MHz center frequency variable delay line was constructed and coherent frequency translation was used to provide operation at X-band. Operating principles for this new intermediate frequency (IF) delay line are presented, and key component issues are discussed. A computer design and analysis tool is described that predicts delay line performance. Experimental results are presented at both the IF and at X-band.**

I. Introduction

IN MANY applications, including radar test and calibration, it is desirable to continuously vary the delay of an electrical signal. For example, consider a radar target simulator that must emulate a scatterer moving radially in range over time relative to the radar. To produce this simulated target, a portion of the radar signal is input into a delay device and the delay is made to match the round trip time of flight for the electromagnetic wave. The output of the delay line is then input into the radar receiver by either directly coupling into the RF receiver or by using a small second antenna to radiate back to the receiver antenna. One necessary feature for such a delay device is a smooth variable delay over a wide tuning range. Currently, no low-cost technologies exist to realize this continuously-variable delay function. Traditional options include the use of multiple fixed delays, tapped delay lines, and digital radio frequency (RF) memories. The last devices utilize analog-to-digital (A/D) converters, digital delays, and digital-to-analog converters to produce the desired delay and the complexity of this approach makes it expensive.

It has been recognized that variable delay lines can be produced using acousto-optics [1]–[4]. These delay devices are based on heterodyne optical detection [1]–[3] and are susceptible to many problems including mechanical and thermal instability, difficulty in manufacturing, and significant phase jitters when the device [1], [2], and [4] is motorized for electronic delay control. These problems are a consequence of using a heterodyne optical system. Recently, Dynetics, Inc. introduced a variable delay line using homodyne optical detection [5]–[7] from a common path configuration. In this approach, both a diffracted optical beam, containing the delayed signal information, and an optical reference beam are made to travel identical paths, thereby removing many instability problems.

In this paper, we describe the development of an acousto-optically implemented delay line. Specific design goals for this variable delay line include X-band operation, low phase noise, coherent operation, 10-MHz instantaneous bandwidth, 1.2 GHz of tunable bandwidth, 45-dB dynamic range, maximum delays greater than 50 μs, and spurious signal suppression greater than 50 dB. In Section II, the theoretical operation of the AO delay line is discussed, and in Section III, the selection of key components is detailed along with analysis of component effects on system performance. In Section IV, the findings from a computer design and analysis tool that accurately predicts delay line performance are presented, and Section V concludes with the presentation of measured device characteristics.

II. If Delay Line Operation

Fig. 1 shows the layout for the AO system that produces a time-delayed replica of an input electrical signal [5], [6]. In operation, an electrical signal is converted into an acoustic signal that propagates at velocity v through the AO interaction medium. A small optical beam is focused at a distance d from the transducer and is modulated and Doppler shifted by the acoustic signal. This Doppler shift should not be confused with that due to the rate of change of delay. The input optical beam is focused into the AO cell, at a normal incidence angle, with a full angle beam convergence given by

$$\theta_{\text{conv}} \geq \frac{1.25 f_{\max} \lambda}{v} \tag{1}$$

where $f_{\max}$ is the maximum frequency input into the delay line AO cell and λ is the optical wavelength [6]. At the AO device, a portion of the optical beam is diffracted and modulated by the input IF signal. Mathematically, the diffracted optical beam, $d(x,t)$, for the $+1$ diffracted order can be written as

$$d(x,t) = A(x-d)s(t-x/v)\exp(j2\pi f_c(t-x/v)) \tag{2}$$

Manuscript received August 18, 1994; revised April 24, 1995. This work was supported in part by Contract DAAH01-93-C-R286 with the U.S. Army Missile Command on Redstone Arsenal, Huntsville, AL.

M. C. Zari is with the Dynetics, Inc., Huntsville, AL USA.

C. S. Anderson is with the University of Florida, Graduate Research Engineering Center, Eglin AFB, FL USA.

W. D. Caraway, III is with the U.S. Army MICOM, Redstone Arsenal, Huntsville, AL USA.

IEEE Log Number 9412684.

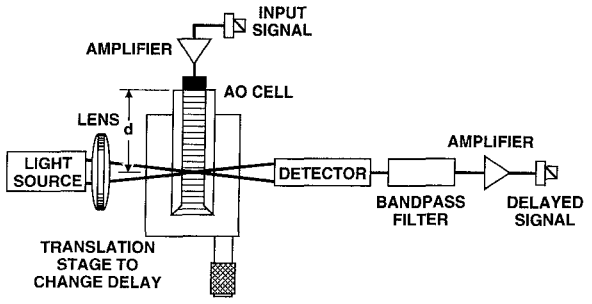

Fig. 1. Layout of variable AO delay line.

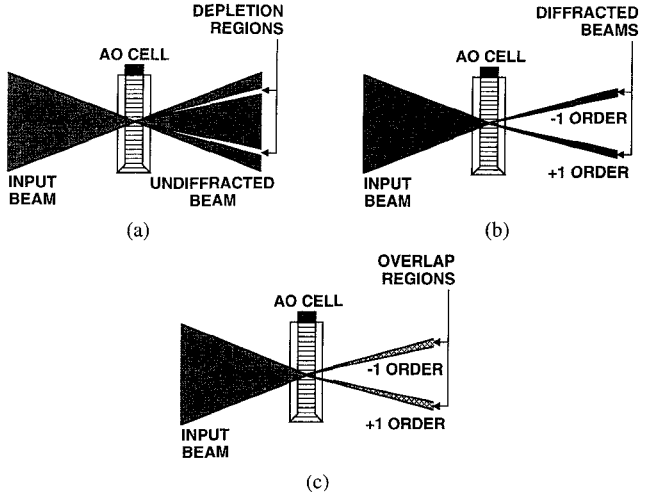

Fig. 2. Homodyne operation of the common-path AO delay line.

where $s(t)$ is the input signal, $A(x)$ is the optical illumination function, and f_c is the center frequency. To recover the electrical signal, a reference optical beam is added to the diffracted signal beam, and the coherent summation of the two beams is square-law detected on a photodetector.

Physically, the reference optical beam is generated from the focused input beam and is always overlapping and collinear with the diffracted beam; these two conditions are important for efficient electrical signal recovery. To illustrate this point, Fig. 2 shows the AO cell output for only the undiffracted light, only the diffracted light, and those regions where the undiffracted and the diffracted beams are overlapping and collinear. In Fig. 2(a), notice that in regions around the plus and minus Bragg angles, some of the light is diffracted as illustrated by the lighter shading in the depletion region. Fig. 2(b) shows that the light diffracted from these regions is shifted in angle by twice the Bragg angle. Thus, light from the upper depletion region [Fig. 2(a)] is shifted to the $+1$ order diffracted beam, and that of the lower depletion region to the -1 order. Fig. 2(c) shows only those regions where the undiffracted and diffracted beams are overlapping and collinear. Because of the focused input laser beam, the undiffracted and diffracted beams remain overlapping and collinear as they leave the device, which is a necessary condition to produce homodyne detection [8]. At the photodetector, the two overlapping beams are coherently summed and square-law detected.

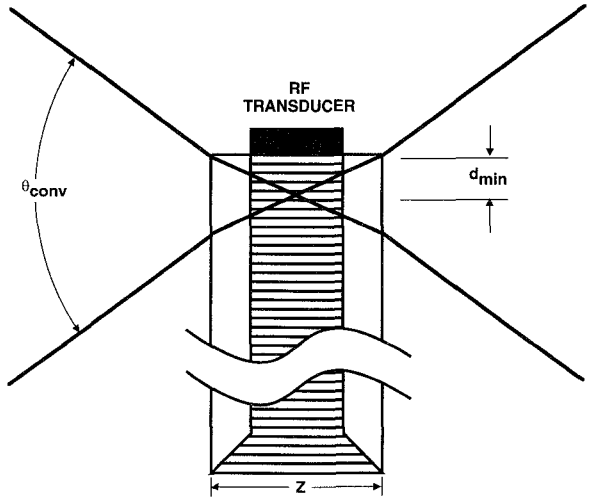

Fig. 3. Minimum time-delay calculation.

At the detector, the square-law detection results in an output photodetector current that is given by

$$i_{\text{det}}(x) \propto \text{Biases} + 2\,\text{Re}\left\{\sum_{-\infty}^{\infty} A^*(x-d)A(x-d) \cdot s(t-x/v)\exp(j2\pi f_c(t-x/v))\,dx\right\} \quad (3)$$

where A is the amplitude of the reference beam. If $I(x)$ has a small spatial extent relative to the resolution size of the signal in the AO cell and can therefore be approximated as a delta function, the output heterodyne signal is simply a time-delayed replica of the input signal and is given by

$$i_{\text{het}}(d) \propto 2\,\text{Re}\{s(t-d/v)\exp(j2\pi f_c(t-x/v))\}. \quad (4)$$

Thus, the time delay is given by the term d/v. The other signal terms in (4) are at baseband and are readily removed with a bandpass filter. By changing the distance d at which the focused optical beam taps the AO cell (e.g., by moving the AO cell with a mechanical translation device), a continuously variable delay line is produced.

III. Component Design Issues

The selection of appropriate components and the mechanical considerations for the delay line determines the final device performance. The major components for the delay line discussed here are the laser diode, the AO cell, and the frequency translation necessary for X-band operation. Each plays a unique role in the RF performance of the finished delay line, thus warranting individual consideration. Also included in this section is an introduction to mechanical and thermal stability issues.

A. Laser Diode

The laser diode provides an unmodulated, collimated light source that is focused into the AO cell through the use of a lens. Wavelength selection is important since it determines the AO cell efficiency, the responsivity of the detector, and

the ease of alignment. We have found that laser diode wavelengths in the range of 670–830 nm are acceptable. Another consideration in laser diode selection is the output power. Since more optical power produces a larger RF output signal, the RF insertion loss of the delay line is reduced. Initially, it appears that the output signal-to-noise ratio (SNR) improves with increasing laser power; however, this is not always true. In tests performed to date, laser relative intensity noise (RIN), caused by rapid intensity fluctuations in the laser, is the dominant noise source. Therefore, as laser power increases, the output noise floor increases proportionately, resulting in no SNR gain.

The anticipated SNR can be calculated by considering the laser noise and the expected output signal power. One common measure of laser diode performance is its RIN, which is defined as

$$\mathrm{RIN} = 10\log\left(\frac{P_{\mathrm{ac}}^2}{P_{\mathrm{dc}}^2}\right) - 10\log(BW) \tag{5}$$

where P_{ac} is the power in the random optical fluctuations from the laser, P_{dc} is the average optical power, and BW is the bandwidth over which the random fluctuations are measured [9]. As defined, the relative intensity noise has units of dB/Hz. Using the square-law relationship for the photodetector, the relative intensity noise can be rewritten in terms of measurable electrical signals as

$$\mathrm{RIN} = \dddot{P}_N - \dddot{P}_{\mathrm{dc}} - 10\log(BW) \tag{6}$$

where $\dddot{P}_N$ is the measured noise power in dBm and $\dddot{P}_{\mathrm{dc}}$ is the measured direct current (dc) power in dBm. The expected SNR from the delay line is directly proportional to the RIN. For this reason, many diodes have been tested for the delay line application. In the frequency ranges of interest (30–200 MHz), we have found visible laser diodes having a RIN as low as −134 dBc/Hz.

B. AO Cell

The design of the AO cell for the variable delay line differs from that of either a point modulator or an AO deflector [10]. Several factors must be balanced during the AO cell design including: 1) bandwidth/center frequency, 2) minimum time delay, and 3) acoustic reflections. Bandwidth and center frequency are almost entirely a function of the AO transducer, which can be designed similar to that used in an AO deflector.

The minimum time delay is an important parameter in the design of some variable delay line devices. The minimum distance, d_{min}, at which the optical probe can be focused from the transducer is a function of the convergence angle of the optical beam and the optical thickness of the crystal. Using the relationship $\tau_{\mathrm{min}} = d_{\mathrm{min}}/v$, the minimum time delay achievable is

$$\tau_{\mathrm{min}} = \frac{Z}{2v}\tan\left(\frac{\theta_{\mathrm{conv}}}{2n}\right). \tag{7}$$

The tellurium dioxide (TeO_2) AO cell selected in this design has a crystal thickness of 6 mm, index of refraction of 2.26, and an acoustic velocity of 617 m/s. From (7) and (8) and the fact that a 150-mrad beam convergence was used, a minimum delay of 161 ns is potentially achievable. However, the selected AO cell has a beveled edge on the transducer side of the crystal to protect it from chipping. As a result, the minimum delay actually achieved was 750 ns.

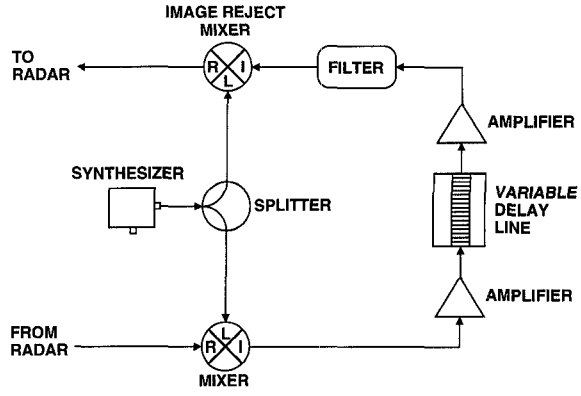

Fig. 4. Simplified block diagram of frequency translation unit.

The final AO cell issue discussed here is multiple time-delayed signals caused by back reflections of the acoustic wave. When this occurs, the acoustic wave propagates to the maximum delay of the crystal, reflects, then modulates the optical beam. Relative to Fig. 1, the measured delay of this component is given by

$$\tau_{\mathrm{double}} = 2T - \frac{d}{v} \tag{8}$$

where T is the total time aperture of the AO cell. For example, in a 54-μs AO cell, a delay set at 10 μs produces a double travel component that is delayed by 98 μs. A combination of techniques is usually employed to reduce double travel effects. First, an acoustic absorber is used at the end of the crystal which reduces the reflected acoustic power by 10–15 dB. Next, the acoustic crystal is cut so that the acoustic reflections are traveling at an angle that is not Bragg-matched to the input focused beam. For our design, cutting the acoustic crystal suppressed acoustic reflections by 40 dB.

C. RF Frequency Translation

To operate the variable delay line at center frequencies other than 33 MHz, a frequency translation unit was used and is shown in the block diagram of Fig. 4. First, the input signal is down converted from RF to the 33-MHz IF of the AO delay line. The IF signal is then time delayed by the variable delay line and frequency translated back to the original center frequency using the same local oscillator.

The ability to achieve tuning at X-band, as well as good phase noise performance, are conflicting requirements. As a compromise, we used a frequency synthesizer having 1.2 GHz of tunability while achieving phase noise levels of −95 dBc/Hz at a 1 kHz offset.

One consequence of using frequency translation is that the input RF signal is no longer true time-delayed. This concept can be seen mathematically. Suppose the input signal is given by

$$s(t) = e(t)\cos(2\pi f_{rf}t + \phi(t)) \tag{9}$$

where $e(t)$ is the envelope of the input waveform, f_{rf} is its center frequency and $\phi(t)$ is a phase modulation. After down conversion to the intermediate frequency (IF), time delay and frequency conversion back to the RF, the output signal can be written as

$$s'_{\mathrm{RF}}(t-\tau) = e(t-\tau)\cos(2\pi f_{rf}[t-\tau]+\phi(t-\tau)+f_{lo}\tau). \quad (10)$$

Notice that both the envelope and phase modulation are delayed by the appropriate amount but the residual phase term $f_{lo}\tau$ remains. At the output, this implies that the phase of the carrier frequency will shift relative to the envelope by a known amount.

When used as a radar target simulator, this non-true time-delay behavior is usually irrelevant because of the fully complex processing that is performed in the radar receiver. The effect of the additional phase term is to cause the signal to move in and out of the in-phase and the quadrature receiver channels. This effectively introduces a Doppler shift that is proportional to the IF. Through appropriate mixing, this can be changed to the desired true Doppler. The processed magnitude, however, is exactly the same and no signal-to-noise loss occurs.

D. Mechanical and Thermal Considerations

During design, care was given to the mechanical and thermal issues including mechanical stability of the AO cell, translation stage repeatability, and thermal expansion of the AO medium. The required mechanical stability of the AO cell mount is determined from

$$\Delta\tau = \frac{\Delta d}{v} \quad (11)$$

where $\Delta\tau$ is the allowable delay variation and Δd is the corresponding allowable distance variation. For example, suppose it is desirable to maintain the phase stability of the delay line to $\pm 30^\circ$. At the 33-MHz center frequency, the delay must be stable to within ± 2.52 ns. Using (11) with an acoustic velocity of 617 m/s, we find that the AO mounting must be stable to within ± 1.56 mm in the acoustic propagation direction; movement in the directions orthogonal to propagation have little effect. This stability can be easily achieved. For this design, the delay was made electronically controllable by using a stepper motor-driven translation stage. Due to stage backlash and other thermal issues, the repeatability is on the order ± 20 ns. This is suitable for the current radar target simulator application. If better phase repeatability were required, a modified mechanical design would be needed.

IV. Computer Design and Analysis Tool

A design and analysis tool has been developed to model the delay line and predict performance prior to device construction. The user inputs specific AO, laser, and lens parameters and the program outputs the frequency response, the insertion loss, and the noise performance. Outputs of the simulation include the predicted frequency response of the delay line as shown in Fig. 5. The uppermost plot is the frequency response at the minimum delay. The lower plot is the frequency response modified by the acoustic attenuation at the maximum delay. From the figure, it is clear that the 10-MHz instantaneous bandwidth is still easily maintained within a 3-dB bound for this design. Other outputs for this design include an output SNR of 57.0 dB, and calculated minimum time delay of 161.4 ns.

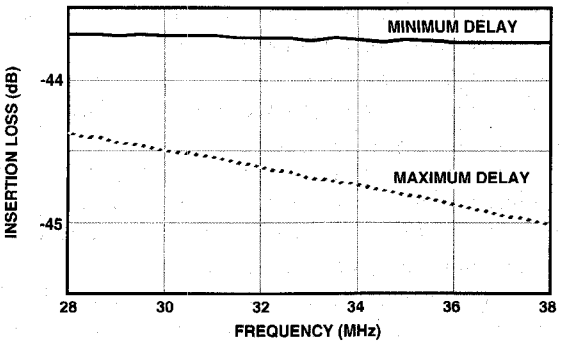

Fig. 5. Predicted frequency response of the variable delay line.

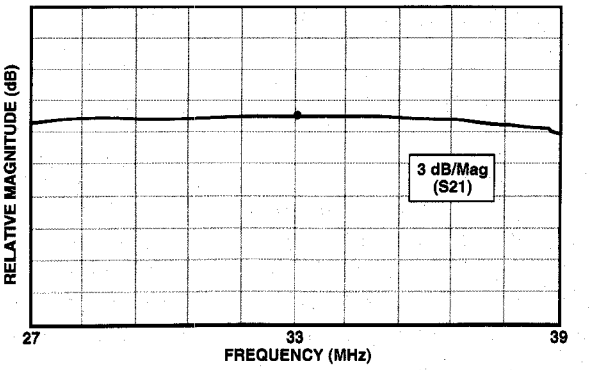

Fig. 6. Frequency response of delay line (12-MHz span) at 33-MHz IF.

V. Delay Line Characterization

Characterization of the AO delay line was performed at the delay line IF (33 MHz) and the RF center frequency (10 GHz). Data presented in this section includes frequency response, time aperture, spur levels, phase noise measurements, and delay variation due to temperature. In addition, system insertion loss as a function of delay is presented.

The measured frequency response of the AO delay line is shown in Fig. 6 for the 33 MHz IF. As seen in the figure, a 3-dB band shape is easily maintained over a 12-MHz bandwidth. This data was taken at a delay of 10 μs. As the delay is changed by moving the AO cell relative to the laser probe, a 3-dB band shape is maintained over the 0.75–54-μs delay range. Although not shown, the phase performance was also measured, and the phase was found to have $\pm 6.5^\circ$ of phase ripple (deviation from linear phase). The insertion loss of the delay line at the RF center frequency, as a function of time delay is also important and is shown in Fig. 7. Notice that the insertion loss variation is within 9.5-dB over the entire delay range. The SNR was measured for the delay line and was

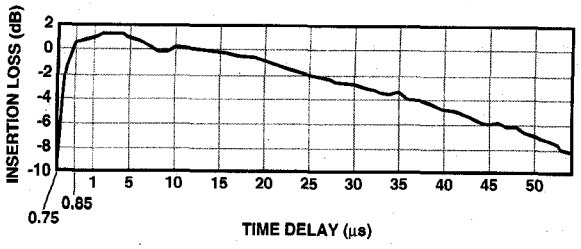

Fig. 7. Insertion loss as a function of time delay ($f_c = 10$ GHz).

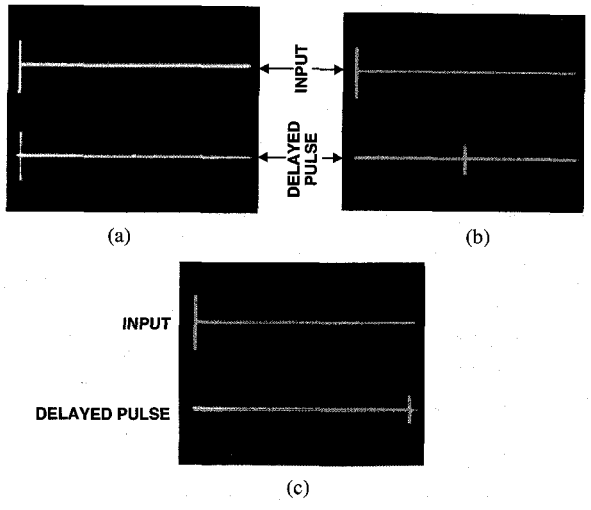

Fig. 8. Delayed output signal. (a) 0.75-μs delay, (b) 25-μs delay, (c) 50-μs delay.

found to be 48 dB rather than the 57 dB that was calculated in Section IV. At this time, the reason for the SNR loss is unclear, but it exceeds the original goal of 45 dB.

Fig. 8 shows the output of the delay line when a 1-μs pulse on a 33-MHz center frequency is input at the IF. The series of figures shows the delayed pulse for three different delays. Using a stepper motor-driven translation stage, and a heating element to maintain the AO cell at 50°C, repeatability was achieved for any desired delay with an accuracy of ±20 ns. When used as a radar target simulator having 10 MHz of bandwidth, the minimum resolvable delay of the radar is 100 ns, which corresponds to a range cell of 15 m. Clearly, the designed delay line can easily position a target within one range cell for most radar systems.

Another feature of interest is the absence of a significant spurious signal production in the frequency domain. Fig. 9 shows the output when a single tone is input into the delay line. Over the 100-MHz bandwidth monitored by the spectrum analyzer, no spurious signals are produced that are greater than −65 dB relative to the desired signal. This clean performance is distinctly superior to that of digital RF memories since these devices produce spurious signals due to the finite accuracy of the digital sampling and reconstruction. Note that spurious signal performance shown in the figure is limited to the signal generator used to perform the test.

For radar test target applications, one of the delay line's most important characteristics is its additive phase noise. Additive phase noise measurements were performed on the

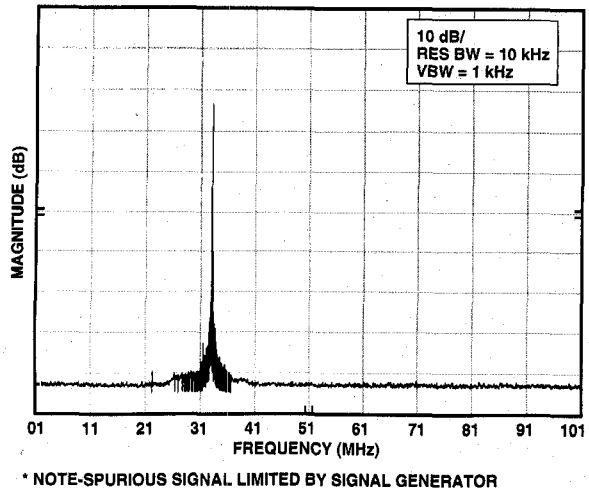

Fig. 9. Spectrum analyzer plot for 33-MHz input tone.

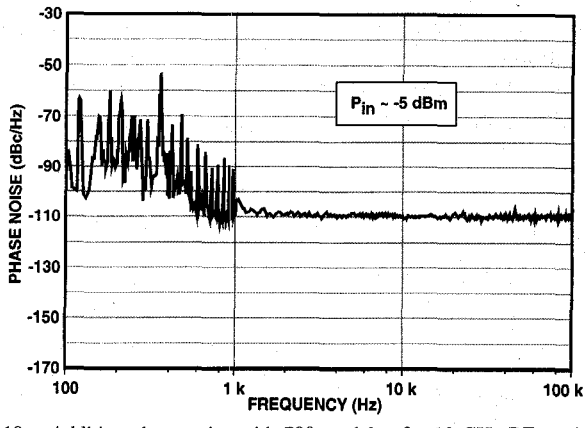

Fig. 10. Additive phase noise with 780 ns delay for 10-GHz RF carrier.

X-Band Delay Line Unit at the RF center frequency. These measurements include the effects from the components of the frequency translation unit and of the delay line. Fig. 10 shows the delay line additive phase noise measurement at 10 GHz. The data shows the additive phase noise of the delay line is below 100 dBc/Hz up to 600-Hz offset from the carrier across the operational band. The frequency spurs seen below 1 kHz are produced primarily by the test set-up and can be traced to 60 Hz multiples and test set-up clocks. A comparison of the phase noise from the test set-up and that of the delay line does show the presence of some 60 Hz-based spurs in the delay line's phase noise; however, these are confined to the region below 360 Hz. Also, an increase in additive phase noise is not expected to change as a function of selected time delay. This is greatly dependent on the stability of the selected synthesizer (see Fig. 4). Overall, the additive phase noise of the delay line is low enough to prevent noise floor degradation in most modern radars when used for target simulation applications.

As mentioned earlier, the delay characteristics of the delay line were measured as a function of temperature. For this test, the delay was set to a nominal value of 54 μs. The temperature was varied over the range of 30–50°C and the

delay was measured on a network analyzer. From the results of this experiment, we calculate that the change in delay is on the order of 180 ppm/°C.

VI. Conclusion

In this paper, we have shown that a high-performance, variable delay line can be produced using AO. The homodyne operation of the delay line allows construction of stable devices. An operational theory has been presented along with the results of a computer simulation to predict performance of the 10-MHz bandwidth delay line. Design considerations for the laser diode, AO cell, and RF translation unit are also discussed. Device characterization has shown that delays ranging between 0.75 and 54 μs can be produced with 48 dB of SNR. When noise and spurious signal performance are compared to more traditional RF delay line approaches, we find them to be competitive. Superior noise and spurious signal performance is obtained when comparing to digital RF memories. However, none of the competing technologies offer the continuous variability of the AO approach. With a slight extension of the technique, multiple tap delay lines could also be produced that would allow for filter construction.

References

[1] A. Browne, "Delay devices for pulse compression radar," *IEEE Conf. Rep. Ser. 20*, pp. 48–56, 1966.

[2] F. Freyre, "Continuously variable delay line," U.S. Patent 4 390 247, 1976.

[3] E. Toughlian and H. Zmuda, "Variable time delay for RF/microwave signal processing," *Proc. SPIE: Optical Technol. Microwave Applicat. V*, vol. 1476, pp. 107–121, Apr. 1991.

[4] R. J. Berinato, "Acousto-optic tapped delay line filter," *Appl. Opt.*, vol. 32, pp. 5979–5809, 1993.

[5] C. Anderson, R. Berinato, M. Zari, and T. Barrett, "Acousto-optics pulls delays to longer lengths," *Microwaves & RF Mag.*, vol. 31, no. 1, p. 117, Jan. 1993.

[6] C. Anderson, R. Berinato, and M. Zari, "Continuously variable delay line," U.S. Patent 5 247 388, 1993.

[7] C. Anderson and M. Zari, "Design and characterization of a 54-μs acousto-optic delay line," SPIE vol. 2240, *Advances in Opt. Inform. Processing VI*, 1994.

[8] A. VanderLugt, *Optical Signal Processing*. New York: Wiley, 1992.

[9] *Laser Diode Operator's Manual, Spectra Diode Labs, Oct. 1991.*

[10] A. Goutzoulis and D. Pape, *Design and Fabrication of Acousto-Optic Devices*. New York: Marcel Dekker, 1994.

Michael C. Zari received the B.E. degree in engineering physics from Stevens Institute of Technology in 1986. He received the M.S.E.E. degree from the University of Alabama in Huntsville in 1990.

He joined Dynetics Inc., where he has designed and developed wide bandwidth AO signal processors for radar applications. He is the Product Manager for Dynetics' delay line products. His current reserach interests are wideband AO signal processors for ESM, radar, and neural network applications as well as the development and product extension of the continuously variable delay line.

Mr. Zari is a member of SPIE and Tau Beta Pi.

Chris S. Anderson began working in optical signal processing while obtaining the Master's degree in engineering science at the University of Florida in 1986. In 1992, he received the Ph.D. in electrical engineering from North Carolina State University

He worked with Dynetics, Inc., where his research interests included research and development of wide bandwidth, AO pulse compressors for imaging radars as wll as adaptive AO and digital equalizers for microwave telecommunications. He was also active in several AO technology developments, including the continuously variable delay line and high speed optical signal processors for radar and ESM applications. Currently, he is an Assistant Professor at the University of Florida Graduate Research and Engineering Center at Eglin AFB.

Dr. Anderson is a member of SPIE and Tau Beta Pi.

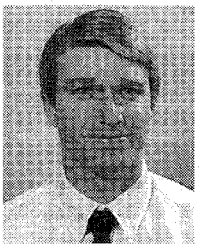

Willie D. Caraway III (S'87–M'87) received the B.E.E. and M.S.E.E. degrees from the Georgia Institute of Technology in 1986 and 1987.

He worked for the U.S. Army Missile Command at Redstone Arsenal in 1981 under the cooperative education program. He has worked as an Antenna and Radar Systems Engineer since 1987. Currently, he serves as a Senior Engineer on the Multi-Role Survivable Radar Program and is the Principle Investigator of the Optical Applications to Radar Program.

Mr. Caraway is a member of Eta Kappa Nu, Tau Beta Pi, and Phi Kappa Phi.